A plasma membrane H^+-ATPase is required for the formation of proanthocyanidins in the seed coat endothelium of *Arabidopsis thaliana*

Ivan R. Baxter*†‡, Jeffery C. Young‡§, Gordon Armstrong§, Nathan Foster§, Naomi Bogenschutz§, Tatiana Cordova¶, Wendy Ann Peer‖, Samuel P. Hazen†, Angus S. Murphy‖, and Jeffrey F. Harper†††**

*Center for Phytoremediation Research and Development, ¶Purdue–UT-Pan American Phytoremediation Program, and ‖Department of Horticulture, Purdue University, West Lafayette, IN 47907; §Department of Biology, Western Washington University, Bellingham, WA 98225; **Biochemistry Department, University of Nevada, MS200, Reno, NV 89557; and †The Scripps Research Institute, La Jolla, CA 92037

Edited by Maarten Koornneef, Max Planck Institute for Plant Breeding Research, Cologne, Germany, and approved December 16, 2004 (received for review August 31, 2004)

The plasma membrane in plant cells is energized with an electrical potential and proton gradient generated through the action of H^+ pumps belonging to the P-type ATPase superfamily. The *Arabidopsis* genome encodes 11 plasma membrane H^+ pumps. Autoinhibited H^+-ATPase isoform 10 (AHA10) is expressed primarily in developing seeds. Here we show that four independent gene disruptions of *AHA10* result in seed coats with a *transparent testa* (*tt*) phenotype (light-colored seeds). A quantitative analysis of extractable flavonoids in *aha10* seeds revealed an ≈100-fold reduction of proanthocyanidin (PA), one of the two major end-product pigments in the flavonoid biosynthetic pathway. In wild-type seed coat endothelial cells, PA accumulates in a large central vacuole. In *aha10* mutants, the formation of this vacuole is impaired, as indicated by the predominance of multiple small vacuoles observed by fluorescence microscopy using a vacuole-specific dye, 5-(and -6)-carboxy 2′,7′-dichlorofluorescein diacetate. A similar vacuolar defect was also observed for another *tt* mutant, *tt12*, a proton-coupled multidrug and toxic compound extrusion transporter potentially involved in loading provacuoles with a flavonoid intermediate required for PA production. The endothelial cells in *aha10* mutants are otherwise healthy, as indicated by the lack of a significant decrease in (*i*) the accumulation of other flavonoid pathway end products, such as anthocyanins, and (*ii*) mRNA levels for two endothelium-specific transcripts (*TT12* and *BAN*). Thus, the specific effect of *aha10* on vacuolar and PA biogenesis provides genetic evidence to support an unexpected endomembrane function for a member of the plasma membrane H^+-ATPase family.

flavonoid | P-type ATPase | proton pump

Proton pumps are used in cells to energize specific membranes with an electrochemical potential and acidify compartments or an extracellular space. In plant cells, three types of proton pumps [P-type, V-type, and pyrophosphatase (PPase)] are all translated on rough endoplasmic reticulum and move through trafficking pathways to provide proton-pumping activity at diverse locations, including the plasma membrane, vacuoles, Golgi, and endosomes. The P-type H^+-ATPases are thought to function exclusively at the plasma membrane (1). The V-type and PPase pumps are most abundant at endomembrane locations and are thought to function primarily in the acidification of vacuoles. Here, we provide genetic evidence for an unexpected function of a plasma membrane P-type H^+-ATPase on an endomembrane system.

The P-type ATPase superfamily has five distinct branches (Fig. 1*a*) and includes pumps that translocate Na^+/K^+, H^+, Ca^{2+}, and heavy metals. They all share a common enzymatic mechanism involving a phospho–aspartate intermediate. The H^+-ATPase branch (P_{3a}) is found in plants and fungi but not in animals. Plants and fungi use H^+-ATPases to energize their plasma membranes with an electrochemical gradient, but animals use a Na^+/K^+-ATPase. In *Arabidopsis* and rice, there are 11 and 10 proton-pump isoforms, respectively, which can be divided into five clusters (2, 3). The functional differences between these clusters have not been determined but may delineate biochemical functions or tissue specificity. The only representative of cluster 3 in *Arabidopsis* is autoinhibited H^+-ATPase isoform 10 (AHA10). This isoform was previously shown to be expressed primarily in the integument layers of developing seeds (4), suggesting a unique seed-specific function.

In the development of the *Arabidopsis* seed, the embryo is nourished and protected by the maternally derived integument layers (5). In early stages of development, transfer cells from the integument are thought to be essential in the source-sink translocation of nutrients. In later stages, integument layers differentiate into a seed coat endothelium that protects the dormant embryo from extreme environmental stresses (e.g., cold, desiccation, and intense sunlight) until conditions are appropriate for germination. One important aspect of this differentiation is the synthesis of flavonoids, which are critical to UV protection, seed coat hardening, and desiccation tolerance (6, 7). In seeds, the two most abundant flavonoid end products are proanthocyanidins (PAs) and anthocyanins, whose biosyntheses diverge after the production of cyanidin (8). Both products accumulate in a large central vacuole within seed coat endothelial cells (9).

The synthesis and function of seed coat flavonoids has been actively investigated in *Arabidopsis* by using forward genetics. Mutations in this pathway have been identified by screening for mutants producing pale-colored seeds [*transparent testa* (*tt*) phenotype] and/or lacking condensed tannins [*tannin deficient seed* (*tds*) phenotype] (10–12). The 15 mapped *tt*/*tds* mutants include six regulatory transcription factors, seven enzymes in the flavonoid biosynthesis pathways, and one GST. Of these 15 mutants, only one (*tt12*) disrupts a membrane transporter. The *TT12* transporter is a member of the multidrug and toxic compound extrusion (MATE) family of transporters (13) and is proposed to function as a H^+-coupled antiporter to load flavonoids (probably an intermediate specific to the PA pathway) into vacuoles within the developing seed coat endothelial cells. Evidence from maize mutants indicates that other flavonoids, such as anthocyanin, are transported into vacuoles or provacuolar compartments through an ATP-binding cassette (ABC)-type transporter (MRP3) (14), which is directly driven by ATP hydrolysis and does not depend on a H^+ gradient across the membrane. At present, the MATE (TT12) and ABC-

This paper was submitted directly (Track II) to the PNAS office.

Abbreviations: AHA10, autoinhibited H^+-ATPase isoform 10; PA, proanthocyanidin; MATE, multidrug and toxic compound extrusion; Ws, Wassilewskija; DMACA, dimethylaminocinnamaldehyde; *tt*, *transparent testa;* T-DNA, transfer DNA; LDOX, leucoanthocyanidin dioxygenase; BAN, banyuls.

‡I.R.B. and J.C.Y. contributed equally to this work.

††To whom correspondence should be addressed. E-mail: jfharper@unr.edu.

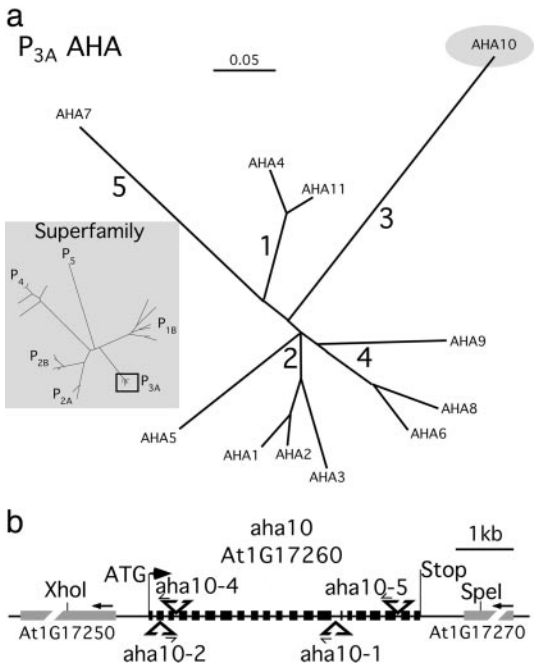

Fig. 1. The *Arabidopsis* P-type ATPase superfamily and map of *AHA10*. (*a*) Relationship tree showing the autoinhibited H^+ P-type ATPase (AHA) family in *Arabidopsis*. The numbers represent the subfamilies of the plant AHAs identified by Arango *et al.* (2) and Baxter *et al.* (3). (*Inset*) Relationship tree showing the subfamilies of plant P-type ATPases identified by Baxter *et al.* (3). A box surrounds the AHA branch shown in the main part of the figure. (*b*) Sites of T-DNA insertions in *aha10* mutants. Exons are shown as black boxes; the coding regions of the two adjacent genes are shown as gray boxes. Arrowheads indicate the direction of transcription. T-DNA insertion points are indicated by triangles, and the left border sequence is shown with arrows. The left border sequences of *aha10–1* ($_{3313}$ATGAAAAATCAcatcccggacgatatattgt) and *aha10–2* (tgactgacagACTTGAAGAG$_{266}$) (*AHA10* sequence in capital letters, numbering from ATG) were determined by sequencing of PCR-amplified borders. The border sequences of *aha10-4* and *aha10-5* can be found at the SIGnAL web site (http://signal.salk.edu/cgi-bin/tdnaexpress). The restriction sites used to create the complementation clone are shown.

type transporter (MRP3) are the only two flavonoid transporters characterized at a genetic level (15).

Here, we report a *tt* phenotype associated with four independent T-DNA (transfer DNA) gene disruptions of *AHA10*, a member of the plasma membrane P-type proton-pump gene family. This *tt* phenotype results from a dramatically reduced accumulation of PA. At present, the only other loss-of-function knockout reported for a plant P-type H^+-ATPase results in pollen lethality (39), supporting the expectation that plasma membrane proton pumps are essential for plant cells (16). In contrast, the *aha10* mutation does not appear to affect the viability of seed coat endothelial cells, suggesting that these cells express other isoforms that provide a genetic redundancy for essential plasma membrane proton-pump functions. Instead, the phenotype of the *aha10* seed coat endothelial cells reveals a specific disruption in (*i*) the maturation of a flavonoid storage vacuole and (*ii*) the accumulation of PA, one of the two most abundant end-product flavonoid pigments. These observations suggest that at least one member of the plasma membrane proton-pump family (i.e., AHA10) has an alternative function in an endomembrane location.

Materials and Methods

Plant Lines and Growth Conditions. Plant lines containing T-DNA insertions in *AtAHA10* (At1g17260) in the Wassilewskija (Ws) background were identified from the Wisconsin collection by PCR screening (*aha10-1* and *aha10-2*) and were confirmed by sequencing (17). Two additional lines in the Columbia (Col) background (*aha10-4*, SALK_019569 and *aha10-5*, SALK_048598.53.35) were obtained from the SIGnAL collection (18) and verified by PCR analysis with the left border primer. Seed for a *tt12* mutant (Ws ecotype) was obtained from the *Arabidopsis* Biological Resource Center (CS5740). Plants were grown in soil under 24-h light conditions in a growth room at 20°C. All experiments were conducted on wild-type and mutant siliques or on seeds from plants that were grown side-by-side in the same soil container.

Complementation. The *AHA10* gene was cloned as an *Xho*I/*Spe*I fragment from a genomic cosmid clone *pcAXA1* (4) into a *pBin* vector (PS249) encoding a glufosinate-ammonium pestanol (BASTA)-resistance gene for plant expression (19). Mutant *aha10-1* plants were transformed by using an *Agrobacterium*-mediated floral dip infiltration method (20). The T1 transgenic plants were selected on 0.5× Murashige and Skoog medium containing 10 μg/ml BASTA.

***p*-Dimethylaminocinnamaldehyde (DMACA) Assay.** Seeds were incubated in 2% (wt/vol) DMACA in 3 M HCl/50% (vol/vol) methanol for 4 days (10). The seeds were then washed four times in 70% ethanol and visualized with a light microscope.

Flavonoid Quantitation. Nonanthocyanin flavonoids were extracted from seeds and analyzed as described in refs. 9 and 10, except that HPLC fractions were separated and analyzed by using a Supelco C18 column on a Waters Alliance 2900S HPLC with diode array monitoring of 200–600 nm. Briefly, the seeds were pulverized and extracted with acetone, Folch-partitioned, and extracted with hexane. For the quantitation of PA, extracts were further subjected to acid hydrolysis in the presence of phloroglucinol (J. T. Baker). Epicatechin analysis was conducted before phloroglucinol hydrolysis, because this hydrolysis releases the terminal epicatechin of the PA polymer. Authentic quercetin, kaempferol, and catechin standards were obtained from Sigma. Cyanidin and pelargonidin were a gift from Dr. Ralph Nicholson (Purdue University), and epicatechin was extracted from black tea (21). Cyanidin-based standards procyanidin B2 and B3 and pelargonidin-based standard pelargonidin chloride for phloroglucinol analysis were obtained from standard collections of Dr. Ralph Nicholson or from ChromaDex (Santa Ana, CA). We did not observe any peaks from *Arabidopsis* PA corresponding to catechin- or pelargonidin-derived adducts. Although the extraction of flavonoids from mature seeds was not complete, as indicated by residual pigment that was recalcitrant to solubilization, the ratios of flavonoids extracted in mature and developing seeds were the same (data not shown). The residual pigment was not extractable with isopropanol, chloroform/methanol/water 1:1:1, or ethyl acetate.

The anthocyanins were extracted from seeds by grinding in methanoic acid and were allowed to sit overnight at 4°C in the dark, Folch-partitioned (22), and analyzed by HPLC as described above.

Visualizing Vacuoles. Vacuoles were observed by using the fluorescent marker 5-(and -6)-carboxy 2′,7′-dichlorofluorescein diacetate (Molecular Probes). Seeds were collected from mature green siliques in which embryos had developed past the torpedo stage (i.e., early mature stage). Seeds were dissected and prepared as described in ref. 9, and images were observed on a Type DM/RB microscope (Leica, Deerfield, IL). A Nikon E5000 digital camera was used to capture images.

Quantitative RT-PCR. Total RNA was extracted from the first 12 green siliques closest to the apical meristem by using RNAEasy kits (Qiagen, Valencia, CA). First-strand cDNA was synthesized by using a poly(dT) primer and Moloney murine leukemia virus reverse transcriptase (Promega) according to the manufacturer's protocol. Taqman assays (Applied Biosystems) were performed on

a Bio-Rad MyIQ Single Color Real Time PCR Detection system (Bio-Rad). Amplification reactions for transcripts encoded by *IPP2* (At3g02780) and *APX3* (At4g35000) were used as normalization controls. The sequences of the primers and probes used are as follows. For quantifying the *BANYULS* (*BAN*) transcript: primers, F1 5′-AGCTTATCTCTCTCGATGTCTTTCATC-3′ and R1 5′-CAGATAGCTTCTGCATTTCCTTGA-3′; probe, 5′-ACCGGT-CACATGCATTTCTTTCCCG-3′. For quantifying the *TT12* transcript: primers, F1 5′-TTGGGATATGCAGTTCATGCTT-3′ and R1 CCCGCTCCTAGCTCATTGC-3′; probe, 5′-TCTAAGTG-CAG CAATCAGTGTGCGAGTG-3′. For quantifying the *APX3* transcript: primers, F1 5′-GCCGTGAGCTCCGTTCTCT-3′ and R1 5′-TCGTGCCATGCCAATCG; probe, 5′-CGCGAACAA-GAACTGTGCTCCTATCATG-3′. For quantifying the *IPP2* transcript: primers, F1 5′-GTATGAGTTGCTTCTCCAGCAAAG-3′ and R1 5′-GAGGATGGCTGCAACAAGTGT-3′; probe, 5′-AAACACAAAGGTTACGTTCCCTCTAGTGTGGACT-3′.

Results

***AHA10* Gene Disruptions.** As part of our effort to determine the *in planta* functions of all 11 *Arabidopsis* AHAs, we identified four independent T-DNA insertion plant lines harboring gene disruptions of *AHA10.* Two lines were obtained in the Ws ecotype from the Wisconsin collection (*aha10-1* and *aha10-2*) (17) and two in the Col ecotype from the Salk collection (*aha10-4* and *aha10-5*) (18) (Fig. 1*b*). Homozygous mutant plants were identified for all four mutations, indicating that the gene disruptions were not lethal. The chromosomal location of this *aha10*/*tt* mutation did not correspond to any well characterized *tt* mutant (23). PCR genotyping of segregating *aha10-2* populations revealed normal Mendelian segregation of the *aha10* mutation ($\chi^2 = 0.644$, $P = 0.7247$, $n = 118$). Extensive phenotypic analysis was restricted to the *aha10-1* and *aha10-2* alleles in the Ws background, although both Col-background mutants showed a similar *tt* phenotype, as described below. The T-DNA insertion site in *aha10-2* was sequenced and shown to be located in a coding sequence exon. The other three *aha10* insertions were located in introns, as determined by border sequences.

Seeds from *aha10* Plants Have a *tt* Phenotype. To assay for phenotypes in *aha10* mutant lines, we conducted a variety of assays for plant growth and development under different growth conditions (see the supporting information, which is published on the PNAS web site). The only consistent difference observed was in seed coat color. Seeds from all four homozygous T-DNA insertion lines had pale seed coats (*tt* phenotype) under all growth conditions tested (Fig. 2 *a* and *b*). This phenotype was not observed in heterozygotes, indicating that all four gene disruptions represent recessive mutations.

The *AHA10* Gene Complements. To confirm that the *tt* phenotype resulted from a loss of *AHA10* function, we transformed *aha10-1* plants with a genomic clone containing the *AHA10* gene with 1.45 kb of upstream sequence and 1 kb of downstream sequence. Seeds from all 11 independent transgenic plant lines had a restored wild-type phenotype, as seen by a visual inspection of seed color as well as by staining for PA using DMACA (data not shown). Because our genomic clone did not contain any other predicted genes, complementation provides strong corroboration that *AHA10* itself is required for normal pigmentation of *Arabidopsis* seed coats.

***aha10* Mutants Have Normal Anthocyanin Levels but Reduced PA.** The first *tt* mutants in *Arabidopsis* defined many of the key enzymes and proteins in flavonoid biosynthesis (11, 12, 24) (Fig. 3). Although the flavonoid pathway produces a wide variety of compounds, colored pigments in the *Arabidopsis* seed coat result primarily from the accumulation of anthocyanins and PA (8). The biosynthesis of both

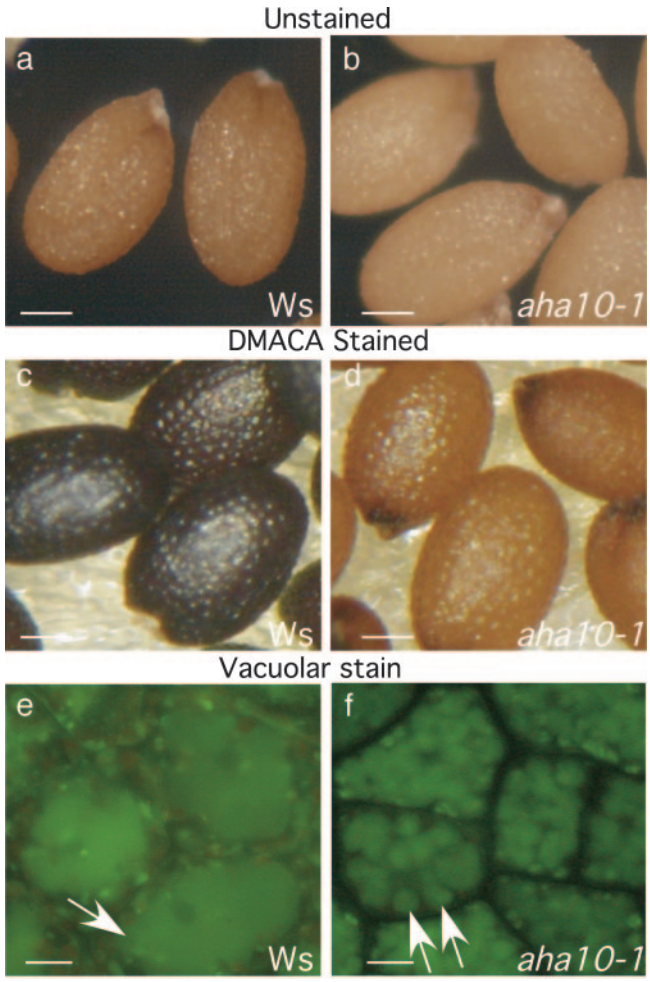

Fig. 2. *AHA10* loss of function results in a *tt* phenotype with reduced PA and altered vacuoles. (*a* and *b*) Light microscope images of wild-type (*a*) and *aha10* (*b*) seeds. (*c* and *d*) DMACA staining of Ws and *aha10-1* seeds. DMACA changes color when it binds to 3′,4′ flavon diols, including PA and its precursors. (*e* and *f*) Seed coat endothelial cells in *aha10* mutants display a vacuolar biogenesis defect. Developing seeds were dissected and stained with the vacuole-specific dye 5-(and -6)-carboxy 2′,7′-dichlorofluorescein diacetate. Arrows in *e* and *f* point to the large and small vacuoles, respectively. (Scale bars: *a–d*, 0.1 mm; *e* and *f*, 10 μm.)

of these end-product pigments includes many shared upstream intermediates but diverges into two specific pathways after the production of cyanidin (Fig. 3).

To determine whether the PA and anthocyanin branches of the pathway were both affected in *aha10* mutants, we quantified extractable levels of anthocyanin and PA in mature seeds. Although wild type and mutants showed comparable levels of anthocyanin, the mutants showed a >100-fold decrease in PA (Table 1). This significant decrease in PA ($P < 0.05$) was confirmed by staining seeds with DMACA (Fig. 2 *c* and *d*), which stains PA much more strongly than it stains other flavonoids. As expected, wild-type seeds stained black, indicating the presence of PA, whereas the *aha10* seeds showed no detectable staining. Thus, *aha10* seeds have a defect in flavonoid production that affects the PA pathway but not the anthocyanin pathway.

A Disruption in PA Production Occurs Downstream of Epicatechin. To delineate the point at which PA production is disrupted in the *aha10* mutants, we analyzed the flavonoid profiles of mature seed extracts by using HPLC. Of the seven extractable flavonoids that were

PLANT BIOLOGY

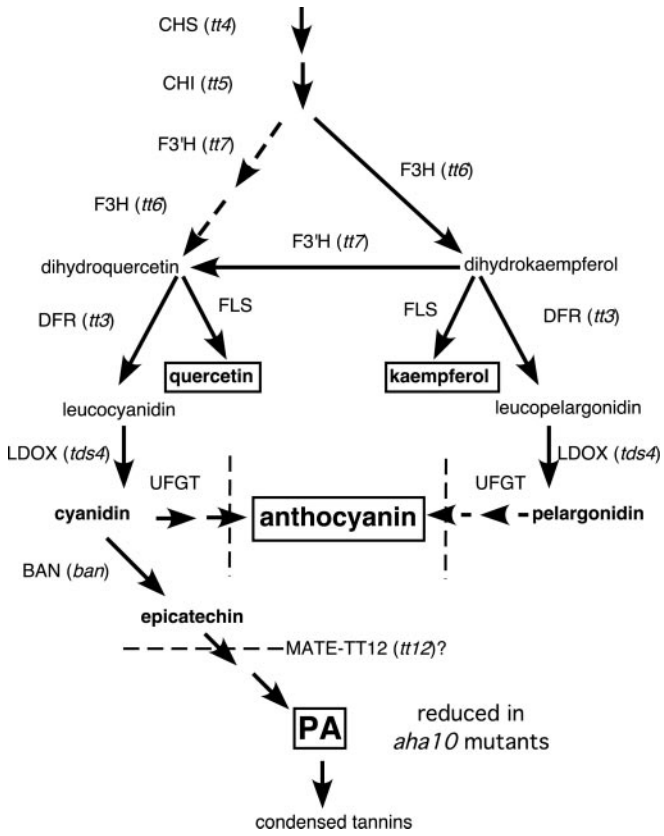

Fig. 3. Flavonoid pathway in *Arabidopsis*. Pathway diagram is derived from ref. 9. The known elements of the flavonoid pathway are indicated. The protein names are capitalized; the corresponding mutant line in *Arabidopsis* is in italics. The different chemical species are indicated in lowercase. Bold letters indicate flavonoids quantified in Table 1. End products are boxed. Dotted line perpendicular to arrow indicates a hypothetical membrane transport step. Plants with disruptions in transcription factor genes TT1, TT2, TT8, TT16, TTG1, and TTG2 have been shown to have *tt* phenotypes, as well. *tds*, *tannin deficient seed*; CHS, chalcone synthase; CHI, chalcone isomerase; F3H, flavone 3 hydroxylase; F3′H, flavone 3′ hydroxylase; DFR, dihydroflavonol reductase; FLS, flavonol synthase; UFGT, UDP glucose-flavonoid 3-*O*-glucosyl transferase.

quantified (Table 1), the end-product PA was the only flavonoid to consistently show a dramatic reduction ($P < 0.05$). In contrast, no significant changes were observed in anthocyanin (discussed above), kaempferol, or pelargonidin ($P > 0.05$). The colorless flavonol quercetin increased slightly ($P < 0.05$). These results provide strong evidence that the primary defect in *aha10* mutants is specific to the PA biosynthetic branch.

In agreement with Abrahams *et al.* (9), we detected only epicatechin from our PA hydrolysis, indicating that *Arabidopsis* PA is composed exclusively of epicatechin monomers. This composition makes cyanidin the intermediate at the branch point that feeds into both the anthocyanin and PA pathways. Because anthocyanin was found at wild-type levels in the mutant, we hypothesized that the levels of the precursor cyanidin would not be reduced in the *aha10* mutant. This expectation was verified, with cyanidin levels actually showing a slight increase (2.7-fold, $P < 0.05$).

In wild type, cyanidin is directly converted to epicatechin (the monomer unit of PA) in the first committed step of the PA pathway (25). This step is catalyzed by the enzyme BAN. To evaluate whether this PA-specific step was normal, we quantified soluble epicatechin directly from seed extracts. No free epicatechin was detectable in wild type, consistent with this intermediate occurring at very low levels. In contrast, significant levels of free epicatechin were detected in the mutants. Thus, the *aha10* defect appears to cause a blockage resulting in the accumulation of epicatechin.

Vacuolar Biogenesis Is Altered in *aha10* and *tt12* Seed Coat Endothelial Cells. PA accumulates in the central vacuole of seed coat endothelial cells (5). To determine whether the loss of AHA10 affects the formation of these vacuoles, we performed microscopy with 5-(and -6)-carboxy 2′,7′-dichlorofluorescein diacetate (Fig. 2 *e* and *f*), a dye previously used to visualize plant vacuoles (9). When developing seeds (in which embryos are in the early mature stage) were examined, a large central vacuole was observed in the wild-type seed coat endothelial cells. In contrast, the equivalent staged cells in *aha10* seeds showed multiple smaller vacuoles. The endothelial cells in Fig. 2 are representative of images most commonly observed for both wild type and mutant. Although small vacuoles were observed in 96% of the mutant endothelial cells ($n = 77$), only 11% of cells from wild-type controls showed comparable morphologies ($n = 64$). As the seeds matured, the differences between wild type and mutant diminished, indicating that the mutation resulted in a developmental delay, as opposed to a complete block in vacuolar biogenesis. We also observed this phenotype in the developing seeds of the *tt12* mutant, where 94% of the cells observed had small vacuoles ($n = 383$).

***aha10* Does Not Reduce the Accumulation of *BAN* and *TT12* mRNA.** To test for an *aha10*-related deficiency in general functions of seed coat endothelial cells, we conducted quantitative RT-PCR for two mRNAs (*BAN* and *TT12*). Both *BAN* and *TT12* are specifically expressed in seed coat endothelial cells and function in the PA-specific branch of flavonoid biogenesis. BAN catalyzes the first committed step in PA synthesis (Fig. 3) (25), whereas *TT12* encodes

Table 1. Quantitation of flavonoids in mature seeds shows mutants with decreased PA

Flavonoids	Ws	*aha10-1*	*aha10-2*	Change from wild type
Kaempferol	0.3 (64)	0.076 (5)	0.10 (21)	Not significant
Quercetin	0.216 (0.07)	0.40 (8)	1.22 (3)	Up ≥1.8-fold
Pelargonidin	0.001 (35)	0.01 (312)	0.001 (137)	Not significant
Cyanidin	0.05 (26)	0.14 (12)	0.27 (23)	Up ≥2.7-fold
Epicatechin				
Pre-PG	0*	0.08 (55)	0.028 (81)	Up
PA EU	12.5 (8)	0.18 (103)	0.10 (47)	Down ≥100-fold
Anthocyanin	7.8 (27)	5.8 (26)	6.2 (9)	Not significant

The levels of each flavonoid are presented with the percent standard deviation in parentheses. Significance determined by Student's *t* test, $P < 0.05$, $n = 3$. PG, phloroglucinol treatment; PA EU, PA extension units (epicatechin-phloroglucinol). All values are in μg of flavonoid/g of seed except anthocyanins, which are expressed as nmol/g of seed.

*No epicatechin was detected in the Ws seed extracts before PG treatment.

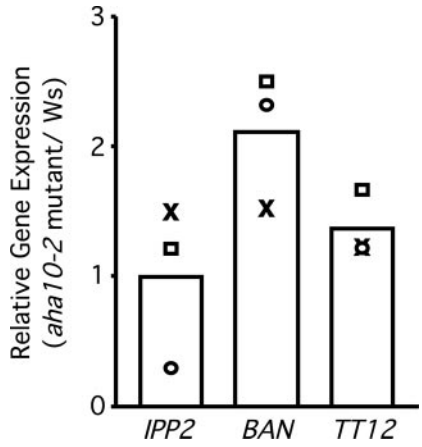

Fig. 4. Expression levels are not decreased for two PA pathway-specific genes. Quantitative RT-PCR of *BAN* and *TT12* transcripts in green siliques. The levels of *BAN*, *TT12*, and a control gene (*IPP2*) were compared with the *APX3* gene for each RNA sample. In controls, the primers for *TT12* and *BAN* were shown to specifically amplify their respective cDNAs from siliques at a level >1,000 times that found by using template RNA from 2-week-old seedling tissue. The relative levels of gene expression are shown as the ratio of mutant to wild type for each transcript. The bars represent the average of three independent trials, which are shown individually as open circles, open squares, and "X"s.

a MATE transporter that potentially functions to transport epicatechin into vacuoles (13). To evaluate the relative expression levels of these two endothelial cell-specific transcripts in mutants and wild type, we compared their expression values with two mRNA transcripts that are expressed in many cell types of the plant (*IPP2* and *APX3*).

The RNA template used for RT-PCR was extracted from the uppermost 12 green siliques located closest to the apical meristem (Fig. 4). In each of three independent experiments, the relative expression levels of *BAN* and *TT12* were slightly higher in the mutant than in the wild type. This finding shows that the expression of these two PA pathway genes is not the rate-limiting step in PA biosynthesis in an *aha10* mutant. More generally, it provides further evidence that the *aha10* disruption does not compromise essential cellular functions (e.g., the plasma membrane electrical potential and proton motive force) that would result in a global decrease in gene expression.

Discussion

***aha10* Disrupts the Biosynthesis of PA.** Evidence presented here shows that four independent homozygous gene disruptions of a plasma membrane proton pump *AHA10* (Fig. 1) all result in a *tt* phenotype (Fig. 2). These mutants appear to result from a loss of AHA10 function, as indicated by the ability to complement *aha10-1* by using an *AHA10* genomic clone. The underlying cause of this *tt* phenotype appears to be related to a 100-fold reduction in PA (Table 1). PA is produced in seed coat endothelial cells and accumulates in large central vacuoles. Because AHA10 is classified as a plasma membrane proton pump, the *aha10*/*tt* phenotype provides an unexpected connection between the function of a putative plasma membrane proton pump and the accumulation of a specific flavonoid in the central vacuole.

Although the exact composition of the colored pigments in the *Arabidopsis* seed coat is unknown, it has been attributed to anthocyanin and PA (8, 13). A complete loss of anthocyanidins and anthocyanins results in a yellow seed, as observed in a chalcone synthase-deficient mutant that produces no flavonoids (24) and the dihydroflavonol 4-reductase mutants that only produce flavonols (26). In contrast, the *aha10* mutants show only a slight reduction in seed color. PA is the only major end-product flavonoid that is missing in *aha10* mutants, suggesting that it is not PA, but anthocyanins or an unextracted pigment, that accounts for the major contribution to seed coat color in *Arabidopsis*.

The *aha10* mutations do not completely eliminate any flavonoid biosynthetic branch in seeds, as evidenced by the detection of all three primary end products of the flavonoid biosynthetic pathway (PA, anthocyanin, and flavonols). Nevertheless, *aha10* dramatically and specifically affects the PA-biosynthetic branch. This phenotype was revealed by the quantitation of seven different extractable seed flavonoids (Table 1). In this analysis, *aha10* mutants showed either no significant change or increased levels of the end products anthocyanin and the flavonols kaempferol and quercetin, in contrast to a 100-fold reduction in the end product PA. Elevated concentrations were also observed for cyanidin, an intermediate that lies at the fork in the branched pathway leading to either PA or anthocyanin. This finding indicates that the defect in *aha10* occurs at a step downstream of cyanidin biosynthesis.

In the downstream conversion of cyanidin to PA, epicatechin is the only known chemical intermediate. The biosynthetic steps leading to epicatechin are posited to occur in the cytosol, although the enzymatic machinery is membrane-attached (27–29). Epicatechin is thought to be the intermediate that is transported into vacuoles (5). Once transported into a vacuole, condensation of epicatechin into PA may occur nonenzymatically in response to an acidic environment (30). In wild type, we did not observe any unpolymerized epicatechin, consistent with it being a low-abundance and transient intermediate. In contrast, we detected significant levels of unpolymerized epicatechin in mutants. This increase in epicatechin is consistent with a pathway "backup" resulting from a block in epicatechin transport into vacuoles or its conversion into PA.

***aha10* and *tt12* Disrupt Vacuolar Biogenesis.** In different plant cells, there can be multiple vacuoles with distinct functions (31, 32). Some plant vacuoles may originate directly from the endoplasmic reticulum; others may require contributions from the Golgi or plasma membrane. Very little is known about the biogenesis of the specialized vacuoles in seed coat endothelial cells (15).

In *aha10* mutants, we observed a predominance of small vacuoles, as opposed to one large central vacuole, in young developing seed coat endothelial cells (Fig. 2). This phenotype appears similar to those observed for gene disruptions of *LDOX* (leucoanthocyanidin dioxygenase) (9) and *TT12*-MATE (shown in this study). LDOX is an oxygenase that converts leucocyanidin to cyanidin. In the *ldox* mutant, the production of downstream flavonoids, such as epicatechin and PA, are blocked, and the endothelial cells develop with an abundance of small vacuoles. Although it is not clear how the *ldox* mutation prevents normal vacuolar biogenesis, two general mechanisms have been proposed. First, the *ldox* mutation may result in the buildup of a toxic upstream intermediate that somehow disrupts vacuolar biogenesis. Alternatively, it may block the production of a downstream intermediate that is required as a positive metabolic trigger for provacuolar maturation. Although the mechanism by which *aha10* and *tt12* disrupt vacuolar biogenesis is also unclear, all three mutations could cause a buildup in the same toxic intermediate or block the synthesis or accumulation of a positive metabolic trigger.

A Model for AHA10's Function in Flavonoid and Vacuolar Biogenesis. Although the expected function of a plasma membrane proton pump is to energize the plasma membrane and thereby enable signaling and solute transport at the cell surface, these established functions do not readily explain the specific vacuolar and PA biosynthesis defects observed for *aha10* mutants. According to the current paradigm, a significant reduction in proton-pump activity at the plasma membrane would result either in cell death or a general down-regulation of all cellular functions. However, three lines of evidence indicate that these established functions were not signif-

icantly impacted by the loss of AHA10. First, the *aha10* mutation was not lethal to seed coat endothelial cells, as evidenced by the production of brown-colored seeds. A lethal effect on this cell layer would be expected to produce a blond-colored seed (5). Second, mutant cells still produced normal or increased levels of non-PA pathway flavonoids, such as anthocyanins and flavonols (Table 1). This observation is most easily explained as a specific block in the PA biosynthesis pathway, rather than a general starvation for initial precursors, which would be expected from a general reduction in nutrient and solute uptake across the plasma membrane. Third, the levels of two seed coat endothelium-specific mRNAs (*BAN* and *TT12*) are expressed at normal to increased levels in the mutant (Fig. 4). Thus, the seed coat endothelial cells in *aha10* mutants appear to have normal plasma membrane functions that supply the cells with adequate nutrients and enable the signaling systems required for their differentiation as pigment-producing cells.

To explain the *aha10* phenotype, we offer a model that posits a unique and direct effect of AHA10 on an endomembrane system. In this model, AHA10 still functions as a proton pump but is recruited from the endoplasmic reticulum or plasma membrane to acidify endosomes or a specific provacuolar compartment. The AHA10-driven acidification may have three consequences. First, acidification may be required to establish a pH gradient and drive uptake ("cargo-loading") of a flavonoid intermediate through a proton-coupled transporter (e.g., possibly epicatechin through the MATE-TT12 transporter). The uptake of PA precursors into vesicles is not only important for compartmentalizing of PA biosynthesis, but also may function to trigger vacuolar maturation. In membrane-trafficking studies, there are many examples in which the loaded "cargo" triggers vesicle maturation or fusion (33, 34). Second, acidification may be required to promote a nonenzymatic conversion of epicatechin to PA. Without this conversion, epicatechin concentrations may reach toxic levels that inhibit vesicle functions, including provacuolar maturation. Third, acidification by itself may be required for proper membrane trafficking, as seen in many endomembrane-trafficking pathways characterized in animal cells (35, 36). Thus, the proposed AHA10-driven acidification of vesicles provides a reasonable hypothesis to explain the *aha10* mutant defects in vacuolar biogenesis and PA biosynthesis.

In mammalian systems, V-type ATPases (proton pumps) drive the acidification of endoplasmic reticulum-derived endomembrane compartments and endosomes originating from the plasma membrane (35–37). For this reason, models for acidification of analogous endomembrane compartments in plants have assumed a similar role for plant V-type ATPase endosomes (38). However, unlike animals, plants also express two additional types of proton pumps, P-type H^+-ATPases and PPases. Thus, it is possible that some combination of these multiple pumps are used throughout the various endomembrane systems in plant cells. Because P-type H^+-ATPases represent the major source of proton pumping at the plant plasma membrane, it is reasonable to hypothesize that such pumps would provide a significant contribution to the proton-pumping capacity of PM-derived endosomal vesicles, some of which we speculate may participate in PA biosynthesis.

Our results do not rule out many alternative models, especially those in which AHA10 has an indirect or unique function not yet assigned to a known proton pump. The working model proposed above provides a logical explanation based on known activities of a proton pump. However, regardless of the mechanism, the *aha10/tt* phenotype is significant because it provides genetic evidence for an unexpected endomembrane function for a member of the plasma membrane proton-pump family. Although it is not clear whether AHA10 is the only member of this family to have an endomembrane function, our results support the hypothesis that some plant cells may use a P-type proton pump to help acidify endosomal or vacuolar compartments, in contrast to animal cells, which rely exclusively on V-type pumps.

We give special thanks to Kathy Truong, Greta Granstedt, and Steve McDowell for technical assistance. This work was supported by grants from the Human Frontier Science Program Organization (RG00268/2000-M to J.F.H.), Department of Energy (DE-FG03-94ER20152 to J.F.H.), National Science Foundation (0077378-DBI to J.F.H., 0132803 to A.S.M., and 0116266 to J.C.Y.), National Institutes of Health (1R01 GM070813-01 to J.F.H.), and Department of Agriculture National Research Initiative (02-35304-12290 to A.S.M.).

1. Sze, H., Li, X. & Palmgren, M. G. (1999) *Plant Cell* **11,** 677–690.
2. Arango, M., Gévaudant, F., Oufattole, M. & Boutry, M. (2003) *Planta* **216,** 355–365.
3. Baxter, I., Tchieu, J., Sussman, M. R., Boutry, M., Palmgren, M. G., Gribskov, M., Harper, J. F. & Axelsen, K. B. (2003) *Plant Physiol.* **132,** 618–628.
4. Harper, J. F., Manney, L. & Sussman, M. R. (1994) *Mol. Gen. Genet.* **244,** 572–587.
5. Debeaujon, I., Nesi, N., Perez, P., Devic, M., Grandjean, O., Caboche, M. & Lepiniec, L. (2003) *Plant Cell* **15,** 2514–2531.
6. Rao, M. V., Paliyath, G. & Ormrod, D. P. (1996) *Plant Physiol.* **110,** 125–136.
7. Li, J., Ou-Lee, T. M., Raba, R., Amundson, R. G. & Last, R. L. (1993) *Plant Cell* **5,** 171–179.
8. Chapple, C. C., Shirley, B. W., Zook, M., Hammerschmidt, R. & Somerville, C. (1994) in *Arabidopsis*, eds. Meyerowitz, E. M. & Somerville, C. (Cold Spring Harbor Lab. Press, Plainview, NY), pp. 989–1030.
9. Abrahams, S., Lee, E., Walker, A. R., Tanner, G. J., Larkin, P. J. & Ashton, A. R. (2003) *Plant J.* **35,** 624–636.
10. Abrahams, S., Tanner, G. J., Larkin, P. J. & Ashton, A. R. (2002) *Plant Physiol.* **130,** 561–576.
11. Debeaujon, I., Leon-Kloosterziel, K. M. & Koornneef, M. (2000) *Plant Physiol.* **122,** 403–414.
12. Koornneef, M., Luiten, W., de Vlaming, P. & Schram, A. (1982) Arabidopsis *Inf. Serv.* **19,** 113–115.
13. Debeaujon, I., Peeters, A. J., Leon-Kloosterziel, K. M. & Koornneef, M. (2001) *Plant Cell* **13,** 853–871.
14. Goodman, C. D., Casati, P. & Walbot, V. (2004) *Plant Cell* **16,** 1812–1826.
15. Grotewold, E. (2004) *Planta* **219,** 906–909.
16. Morsomme, P., Slayman, C. W. & Goffeau, A. (2000) *Biochim. Biophys. Acta* **1469,** 133–157.
17. Young, J. C., Krysan, P. J. & Sussman, M. R. (2001) *Plant Physiol.* **125,** 513–518.
18. Alonso, J. M., Stepanova, A. N., Leisse, T. J., Kim, C. J., Chen, H., Shinn, P., Stevenson, D. K., Zimmerman, J., Barajas, P., Cheuk, R., *et al.* (2003) *Science* **301,** 653–657.
19. Becker, D., Kemper, E., Schell, J. & Masterson, R. (1992) *Plant Mol. Biol.* **20,** 1195–1197.
20. Clough, S. J. & Bent, A. F. (1998) *Plant J.* **16,** 735–743.
21. Bailey, R., Nursten, H. & McDowell, I. (1993) *J. Sci. Food Agric.* **63,** 455–464.
22. Adamse, P., Peters, J., Jaspers, P., van Tuinen, A., Koornneef, M. & Kendrick, R. (1989) *Photochem. Photobiol.* **50,** 107–111.
23. Sagasser, M., Lu, G. H., Hahlbrock, K. & Weisshaar, B. (2002) *Genes Dev.* **16,** 138–149.
24. Shirley, B. W., Kubasek, W. L., Storz, G., Bruggemann, E., Koornneef, M., Ausubel, F. M. & Goodman, H. M. (1995) *Plant J.* **8,** 659–671.
25. Xie, D. Y., Sharma, S. B., Paiva, N. L., Ferreira, D. & Dixon, R. A. (2003) *Science* **299,** 396–399.
26. Shirley, B. W., Hanley, S. & Goodman, H. M. (1992) *Plant Cell* **4,** 333–347.
27. Xie, D. Y., Sharma, S. B. & Dixon, R. A. (2004) *Arch. Biochem. Biophys.* **422,** 91–102.
28. Saslowsky, D. & Winkel-Shirley, B. (2001) *Plant J.* **27,** 37–48.
29. Burbulis, I. E. & Winkel-Shirley, B. (1999) *Proc. Natl. Acad. Sci. USA* **96,** 12929–12934.
30. Marles, M. A., Ray, H. & Gruber, M. Y. (2003) *Phytochemistry* **64,** 367–383.
31. Paris, N., Stanley, C. M., Jones, R. L. & Rogers, J. C. (1996) *Cell* **85,** 563–572.
32. Surpin, M. & Raikhel, N. (2004) *Nat. Rev. Mol. Cell. Biol.* **5,** 100–109.
33. Aridor, M. & Traub, L. M. (2002) *Traffic* **3,** 537–546.
34. Petäjä-Repo, U., Hogue, M., Bhalla, S., Laperrière, A., Morello, J. P. & Bouvier, M. (2002) *EMBO J.* **21,** 1628–1637.
35. Gu, F. & Gruenberg, J. (2000) *J. Biol. Chem.* **275,** 8154–8160.
36. Zeuzem, S., Zimmermann, P. & Schulz, I. (1992) *J. Membr. Biol.* **125,** 231–241.
37. Nishi, T. & Forgac, M. (2002) *Nat. Rev. Mol. Cell. Biol.* **3,** 94–103.
38. Nebenfuhr, A., Ritzenthaler, C. & Robinson, D. G. (2002) *Plant Physiol.* **130,** 1102–1108.
39. Robertson, W. R., Clark, K., Young, J. C. & Sussman, M. R. (2004) *Genetics* **168,** 1677–1687.